A Spectral Nudging Technique for Dynamical Downscaling Purposes

HANS VON STORCH, HEIKE LANGENBERG, AND FRAUKE FESER

Institute of Hydrophysics, GKSS Research Centre, Geesthacht, Germany

(Manuscript received 21 June 1999, in final form 1 January 2000)

ABSTRACT

The ''spectral nudging'' method imposes time-variable large-scale atmospheric states on a regional atmospheric model. It is based on the idea that regional-scale climate statistics are conditioned by the interplay between continental-scale atmospheric conditions and such regional features as marginal seas and mountain ranges. Following this ''downscaling'' idea, the regional model is forced to satisfy not only boundary conditions, possibly in a boundary sponge region, but also large-scale flow conditions inside the integration area.

In the present paper the performance of spectral nudging in an extended climate simulation is examined. Its success in keeping the simulated state close to the driving state at larger scales, while generating smaller-scale features is demonstrated, and it is also shown that the standard boundary forcing technique in current use allows the regional model to develop internal states conflicting with the large-scale state. It is concluded that spectral nudging may be seen as a suboptimal and indirect data assimilation technique.

1. Background

The state of the atmosphere cannot be observed in its entirety. Only samples of mostly point observations irregularly distributed in space are available. They are used by operational weather centers to construct, or ''analyze,'' a continuous distribution of atmospheric variables. Such analyses are our best guess of the atmospheric state and deviate from the true, unknown state to some extent. Likely, the large scales are best described, simply because they are better sampled. On the other hand, the details on scales of a few tens of kilometers and less are insufficiently sampled and subject to significant uncertainty.

In the past, the analyses were prepared by hand. The major breakthrough was the systematic interpretation of observational data aided by quasi-realistic dynamical models. However, the only features that can be well reproduced by these objective analyses with quasi-realistic models are those that are well resolved by the model. For example, while the effect of the Baltic Sea may to some extent be captured, the imprint of Jutland, separating the Baltic Sea from the North Sea, may not. Thus, the missing details in analyses remains at present a major problem in weather analyses.

While in days gone by the purpose of weather, or synoptic, analyses was for preparing short-term weather forecasts, these analyses have in recent years attained a different role, namely to provide a database for climatic and other environmental studies (von Storch et al. 2000). For fulfilling this purpose, it is no longer sufficient to have the best analysis at a given day. It is also necessary that the quality of the analyses is homogeneous, so that improvements in the analysis process do not introduce artificial signals in the climate dataset. For meeting these requirements, weather services have prepared so-called global reanalyses; that is, they have analyzed weather observations of the past decades with the same analysis scheme (Kalnay et al. 1996).

We suggest the ''spectral nudging'' technique (Waldron et al. 1996) for using these global reanalyses to derive smaller-scale analyses. This technique is based on the view that small-scale details are the result of an interplay between larger-scale atmospheric flow and smaller-scale geographic features such as topography, land–sea distribution, or land use (von Storch 1999). To describe this small-scale response, a regional climate model is forced with large-scale weather analyses. Differently from the conventional approach, the forcing is not only stipulated at the lateral boundaries but also in the interior. This interior forcing is maintained by adding nudging terms in the spectral domain, with maximum efficiency for large scales and no effect for small scales. Also, the nudging is confined to higher altitudes, so that the atmospheric state at lower levels is free to adjust to surface geographical properties. Waldron et al. (1996) named the technique spectral nudging. As far as we know this technique has not been used in regional climate simulations, but it shares similarities with methods

Corresponding author address: Dr. Hans von Storch, Institute of Hydrophysics, GKSS Research Centre, Max-Planck-Straße, D-21502 Geesthacht, Germany.
E-mail: lehmannn@gkss.de

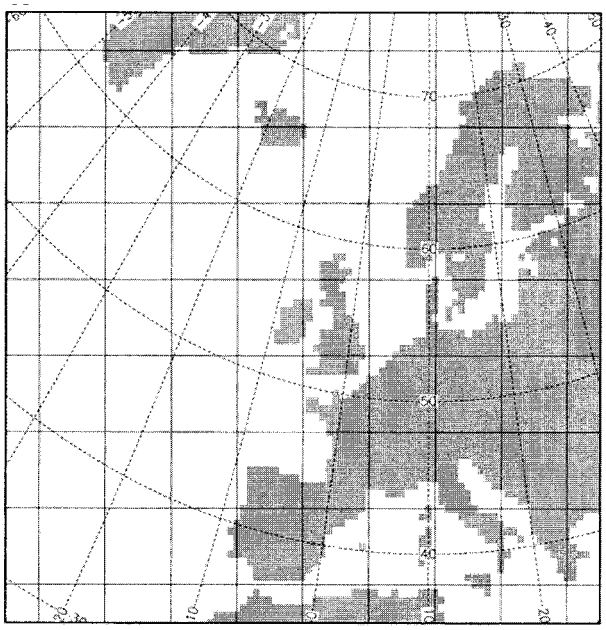

FIG. 1. The model area and the REMO grid. Solid lines demarcate 100 (10 × 10) grid boxes. Because of the spherical resolution, the straight lines are only approximations.

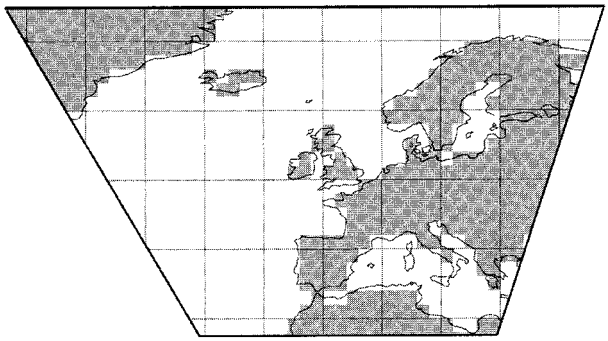

FIG. 2. The REMO model domain and the NCEP grid. The lines demarcate every fifth grid box.

that force area averages upon the interior solution as proposed by Kida et al. (1991), Sasaki et al. (1995), and McGregor et al. (1998), or the technique to insert the large-scale state (Juang and Kanamitsu 1994; Juang et al. 1997; Cocke and LaRow 2000) into the spirit of ''anomaly models'' (Navarra and Miyakoda 1988). A conceptually similar technique has been used to impose a prescribed tropospheric state on an upper-atmosphere model (Kouker et al. 1999).

For purposes of weather analysis, our proposed technique is suboptimal. Ideally, inside the model area one would directly assimilate local observational data, which had little impact on the coarse-grid global reanalyses and, accordingly, were not fully exploited. However, such a scheme is technically very demanding and often not feasible. The proposed technique may be considered a ''poor person's data assimilation technique.''

The same technique may be used to derive regional-scale climate change scenarios from global climate models [''downscaling''; von Storch (1995)]. The basic idea of downscaling is to transfer onto smaller scales that large-scale information which has been simulated reliably in climate change scenarios. This is done with the help of statistical models or dynamical regional climate models. The latter technique, named dynamical downscaling, uses output from global climate models to force regional atmospheric (e.g., Giorgi 1990; Podzun et al. 1995; Jacob and Podzun 1997; Kidson and Thompson 1998; Rinke and Dethloff (2000)) or regional oceanic model (Kauker 1998). In nearly all studies performed to date, the forcing is administered exclusively at the lateral boundaries. The technique of statistical dynamical downscaling developed by Fuentes and Heimann (1996) and Frey-Buness et al. (1995) is related to our approach, as they consider the response of a regional climate model to prescribed conditions such as the geostrophic wind.

In our view, the conventional practice of using forcing exclusively along the lateral boundaries stems from the classic view of regional weather modeling as being a boundary problem rather than a downscaling problem. Problems like data assimilation and downscaling were not considered in classical numerical mathematics. The inclusion of the ''sponge zone'' (Davies 1976) was already a violation of the ''pure'' mathematical concept. In this paper we demonstrate that the boundary value format is conceptually inappropriate for the problem at hand.

The present paper is organized as follows. A brief introduction of the regional atmospheric model is given in section 2. The spectral nudging technique is described in section 3, and the results are presented and discussed in section 4. The discussion makes use of measures, which quantify the degree of similarity or dissimilarity on different spatial scales. Sensitivity experiments dealing with the strength of the coupling are considered. Conclusions are summarized in section 5.

2. REMO model

We use the regional climate model REMO as described by Jacob and Podzun (1997). REMO is a grid-point model featuring the discretized primitive equations in a terrain-following hybrid coordinates system. Details are given by Jacob and Podzun (1997) and Jacob et al. (1995). The finite-differencing scheme is energy preserving. The prognostic variables are surface air pressure, horizontal wind components, temperature, specific humidity, and cloud water. A soil model is added to account for soil temperature and water content.

The integration area shown in Fig. 1 has a horizontal spherical resolution of 0.5° with a pole at 35°N, 170°W, resulting in 91 × 81 grid points. Because of the spherical

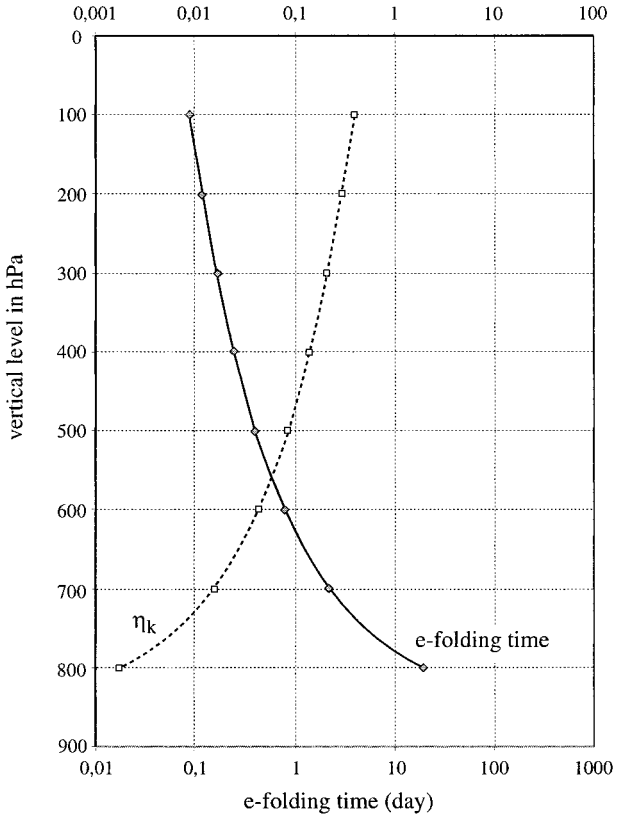

FIG. 3. Vertical distribution of the spectral nudging term η^0 (dashed line) and corresponding *e*-folding time in days (solid line).

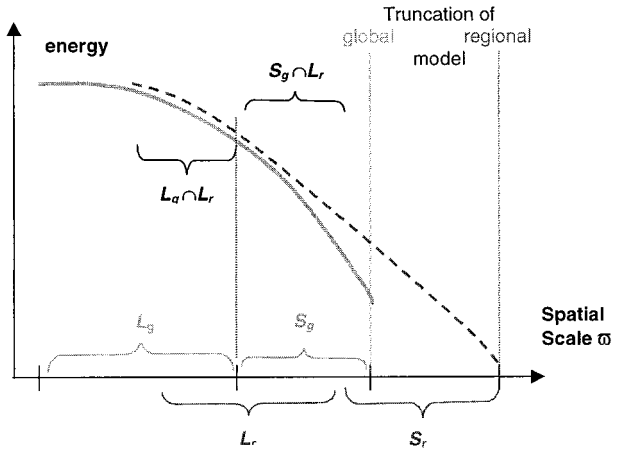

FIG. 4. Sketch of spatial ranges $\mathcal{L}$ and $\mathcal{S}$ of global analyses and regional model.

resolution, the straight grid lines shown in the map are only approximate. A time step of 5 min is adopted.

REMO is forced with National Centers for Environmental Prediction (NCEP) reanalyses (Kalnay et al. 1996) over the 3-month period of January–March 1993. These observed states are updated every 6 h. In between, values are derived through linear interpolation. The horizontal resolution of the analyses is approximately 2° longitudinally and latitudinally (Fig. 2). Since REMO operates with a rotated spherical grid, its coverage with NCEP grid boxes is inhomogeneous. There are 21 NCEP boxes in the north–south direction. In the east–west direction, there are 27 boxes along the southern margin and 48 along the northern margin. That is, the REMO model offers a resolution enhanced by factor of 1:16, on average. Maximum improvement of resolution is achieved in the southern part of the integration area.

3. Spectral nudging

As outlined in the introduction, we have used two different approaches to force the regional model to follow the steering provided by the analyses. In the ''standard'' approach in current use, the steering takes place exclusively along the lateral boundaries in the spirit of a classical boundary value problem. In the spectral nudging approach, the atmospheric state inside the integration area is also forced to accept the analyses for large scales whereas smaller scales are left to be determined by the regional model.

In the standard setup (Jacob and Podzun 1997), the observed state is forced upon the model in a lateral boundary zone covering eight grid points using Davies's (1976) classical ''sponge'' technique: The ''interior'' solution of the model, denoted Ψ, is brought closer to, or ''nudged'' to the observed state, denoted Ψ^*, by adding an adjustment or restoring term $\gamma \cdot (\Psi^* - \Psi)$, where the ''nudging coefficient'' γ takes largest values at the lateral boundary and decreases toward the interior of the integration domain. When $\Psi > \Psi^*$, the restoring terms cause a decrease in Ψ, and when $\Psi < \Psi^*$ an increasing tendency of Ψ is induced. The nudging coefficient has units of s^{-1}. This standard approach is commonly used in regional weather forecasting and regional climate simulations. The sponge zone has been introduced to avoid reflection of traveling features at the boundaries. Inconsistencies stemming from internally generated features traveling toward the lateral boundaries and conflicting there with the prescribed conditions are dampened out in this manner.

In the spectral nudging approach, the lateral ''sponge forcing'' is kept and an additional steering is introduced as described next.

Consider the expansion of a suitable REMO variable:

$$\Psi(\lambda, \phi, t) = \sum_{j=-J_m, k=-K_m}^{J_m, K_m} \alpha_{j,k}^m(t) \exp(ij\lambda/L_\lambda) \exp(ik\phi/L_\phi) \quad (1)$$

with zonal coordinates λ, zonal wavenumbers j, and zonal extension of the area L_λ. Meridional coordinates are denoted by ϕ, meridional wavenumbers by k, and the meridional extension by L_ϕ. Also, t represents time. For REMO, the number of zonal and meridional wavenumbers is J_m and K_m. A similar expansion is done for

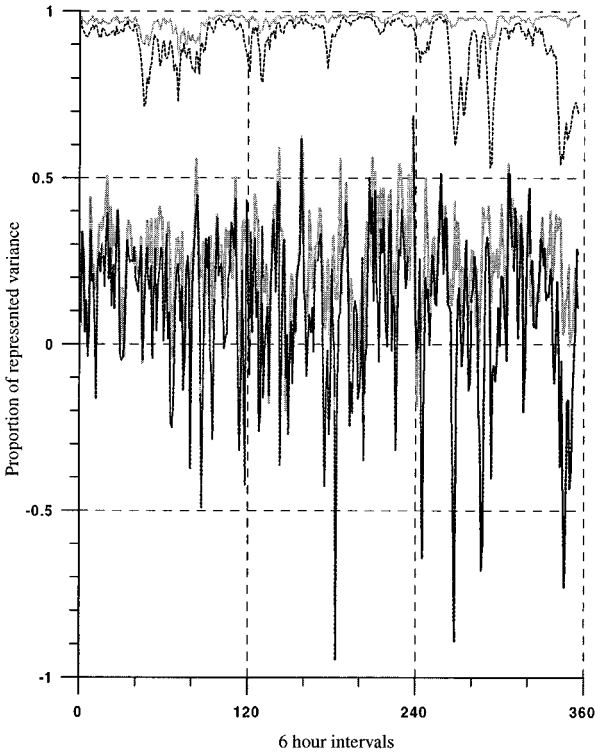

FIG. 5. Measures of similarity $\mathcal{P}_g(t)$ (upper curves) and $\mathcal{P}_r(t)$ (lower curves) for the meridional wind at 500 hPa for the boundary forcing (black lines) and the spectral nudging (gray lines) simulation.

the analyses, which are given on a coarser grid. The coefficients of this expansion are labeled $\alpha^a_{j,k}$, and the number of Fourier coefficients is $J_a < J_m$ and $K_a < K_m$. The confidence we have in the realism of the different scales of the reanalysis depends on the wavenumbers j and k and is denoted by $\eta_{j,k}$.

The model is then allowed to deviate from the state given by the reanalysis conditional upon this confidence. This is achieved by adding nudging terms in the spectral domain in both directions:

$$\sum_{j=-J_a,k=-K_a}^{J_a,K_a} \eta_{j,k}[\alpha^a_{j,k}(t) - \alpha^m_{j,k}(t)] \exp(ij\lambda/L_\lambda) \exp(ik\phi/L_\phi). \tag{2}$$

In the following, we will use the nudging terms dependent on height. That is, our confidence in the reanalysis increases with height. On the other hand, we leave the regional model more room for its own dynamics at the lower levels where we expect regional geographical features are becoming more important. The better the confidence, the larger the $\eta_{j,k}$ values and the more efficient the nudging term.

In this study, we have applied nudging to the zonal and meridional wind components. Following Giorgi et al. (1993) we use a height-dependent nudging coefficient. Specifically, we use the prescription of the German Weather Service version of REMO, which uses a pointwise nudging in case of excessively high wind speeds for preventing numerical instability,

$$\eta^0(p) = \begin{cases} \alpha\left(1 - \dfrac{p}{850\ \text{hPa}}\right)^2 & \text{for } p < 850\ \text{hPa} \\ 0 & \text{for } p > 850\ \text{hPa} \end{cases} \tag{3}$$

with p denoting pressure (Doms et al. 1995). In our base simulation with spectral nudging we used the ad hoc value $\alpha = 0.05$, resulting in a vertical profile as shown in Fig. 3. This choice amounts to an e-folding decay time of an introduced disturbance of about 20 days at 800 hPa, 10 h at 500 hPa, and about 3 h at 100 hPa. (The e-folding time is given by $\Delta t/\eta$ with $\Delta t = 300$ s.)

We have set $\eta_{j,k} = \eta^0$ for $j = 0 \ldots 3$ in the north–south direction, $k = 0 \ldots 5$ in the east–west direction, and $\eta_{j,k} = 0$ otherwise. That is, wavelengths of about 15° and larger are considered to be reliably analyzed by NCEP, corresponding to six and more NCEP grid points. More elaborate specifications could certainly have been used. However, some sensitivity experiments indicated that the effect would be somewhat marginal (see below).

TABLE 1. Averaged variances for the different spatial scales for zonal and meridional wind components at 850 hPa.

Scale/variable	Units $m^2\ s^{-2}$	NCEP analyses	REMO standard	REMO nudging
Zonal wind				
$\mathcal{L}_g$	10^{-2}	1.6	1.2	1.6
$\mathcal{S}_g \cap \mathcal{L}_r$	10^{-6}	3.7	7.7	8.1
Meridional wind				
$\mathcal{L}_g$	10^{-2}	1.4	1.3	1.5
$\mathcal{S}_g \cap \mathcal{L}_r$	10^{-6}	2.1	6.5	8.5

4. Results

We demonstrate in section 4a that spectral nudging successfully prevents the regional model from deviating from the given large-scale state. We also show that significant deviations take place when the standard approach is used. In section 4b, a comparison with station data reveals that the spectral control is limited to the largest scales, so that the representation of the local time series is indeed improved compared to the NCEP reanalyses and the REMO standard run. In section 4c, a number of sensitivity experiments is presented and discussed.

a. Efficiency of large-scale control

We divide the spectral domain into several intervals. We assume that both the regional and global model have two spectral domains: a large-scale domain, $\mathcal{L}$, and a small-scale domain, $\mathcal{S}$. The model has different skills in the domains $\mathcal{L}$ and $\mathcal{S}$ to realistically analyze or simulate the real state. Only the results in $\mathcal{L}$ are considered re-

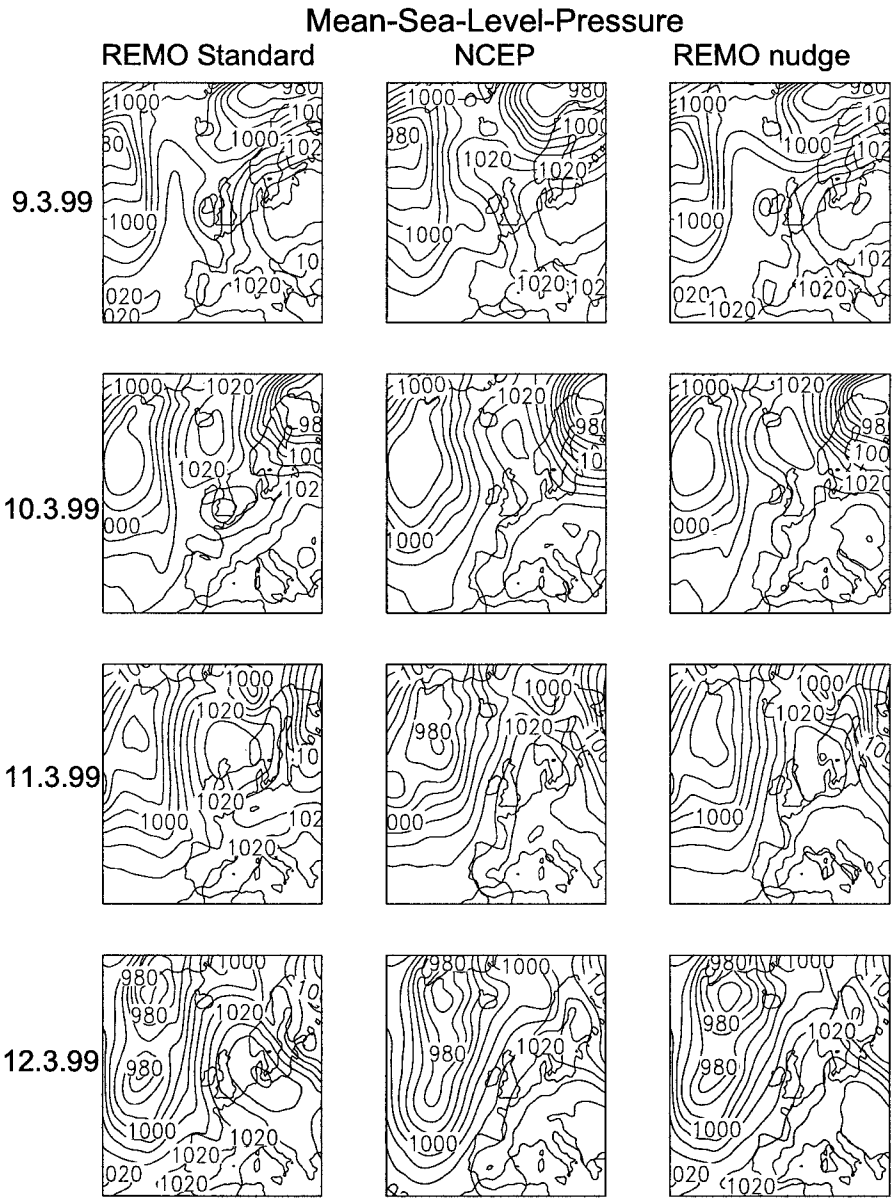

FIG. 6. An episode with large differences between the standard run and the spectral nudging run: 9–12 Mar 1993. Mean sea level air pressure distribution: (left) boundary forcing run, (middle) NCEP analyses (input), (right) spectral nudging. Spacing equals 5 hPa.

liable. So far there is no objective way to identify the interval $\mathcal{L}$, but it is often believed that the largest wavenumber in $\mathcal{L}$ is several mesh sizes of the model's grid. Since the global model and the regional model have different grids, their ''reliable'' domains, $\mathcal{L}_g$ and $\mathcal{L}_r$, are different (Fig. 4). In $\mathcal{L}_g \cap \mathcal{L}_r$ the results of the regional model should not deviate from the global analyses, as the results of $\mathcal{L}_g$ are considered skillful. Therefore, for these scales, large values of η_k are adopted. However, in the domain $\mathcal{S}_g \cap \mathcal{L}_r$ significant modifications are expected and wanted, because the regional model has the role of adding detail in these spatial scales. Accordingly, the nudging term η_k is set to zero for these scales.

We measure the similarity of input NCEP fields and output REMO fields at time t by the proportion of spatial variability of the output described by the input:

$$\mathcal{P}(t) = 1 - \frac{\langle [\Psi(t) - \Psi^*(t)]^2 \rangle}{\langle \Psi(t)^2 \rangle}, \tag{4}$$

where $\Psi(t)$ is the output REMO field at time t, Ψ^* the input NCEP field, and $\langle \cdot \rangle$ a spatial average. When this averaging is done for scales $\omega \in \mathcal{L}_g \cap \mathcal{L}_r$, we denote

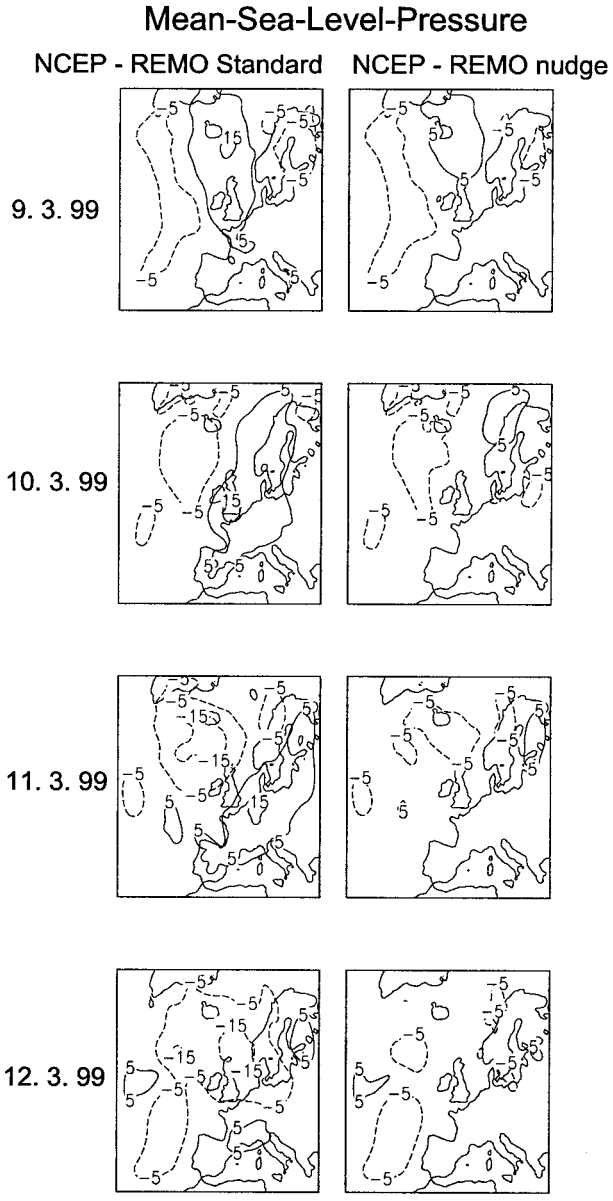

FIG. 7. Mean sea level air pressure differences NCEP minus (left) boundary forcing run and (right) spectral nudging run. Spacing equals 10 hPa.

the similarity measure as $\mathcal{P}_g$. This number should be close to one, as we do not want to modify the scales reliably described by the NCEP analysis. However, for the spectral domain $\mathcal{S}_g \cap \mathcal{L}_r$, we do not request the REMO field to be similar to the input fields, so that the measure of similarity $\mathcal{P}_r$ may be much smaller than 1.

In the present analysis, the set $\mathcal{L}_g \cap \mathcal{L}_r$ comprises zonal wavenumbers up to $k \leq 5$ and meridional wavenumbers $j \leq 3$, so that for all $(j, k) \in \mathcal{L}_g \cap \mathcal{L}_r$ $\eta_{j,k} = \eta^0$. The domains $\mathcal{S}_g \cap \mathcal{L}_r$ contains $5 < k \leq 13$ and $3 < j \leq 10$ so that $\eta_{j,k}$ is zero for these scales. Note that the exact definition of these sets is inconsequential for the performance of the nudging technique as the numbers $\mathcal{P}_g$ and $\mathcal{P}_r$ are diagnostics; in fact, the diagnostic results are rather insensitive to the details of this choice.

The time series of the similarity measures, $\mathcal{P}_g$ and $\mathcal{P}_r$, calculated for both the standard run and the spectral nudging run, have been calculated for relative humidity and temperature as well as for the zonal and meridional wind components at 850 and 500 hPa. As the nudging is applied to velocity only, the effect is strongest in these variables, whereas the difference is significant but somewhat less dramatic in terms of temperature or humidity (not shown). For the sake of brevity results are shown only for the meridional wind at 500 hPa in Fig. 5: in the spectral nudging run $\mathcal{P}_g$ hardly deviates from the ideal value of 1 whereas in the boundary forcing run for the values less than 1 sometimes as low as 0.6 are obtained (Fig. 5). The $\mathcal{P}_r$ values between 20% and 40% indicate that REMO considerably modifies the scales that had been insufficiently resolved by NCEP. For the most part, $\mathcal{P}_r$ is somewhat smaller for the standard boundary forcing run; that is, controlling the large-scale features in $\mathcal{L}_g r$ has some effect on $\mathcal{S}_g \cap \mathcal{L}_r$ as well.

The other relevant measure is the variance for the different spectral domains: the variances in $\mathcal{S}_g \cap \mathcal{L}_r$ are similar in both regional simulations. This is exemplified by Table 1 listing averaged variances for the different spatial scales for the zonal and meridional wind components at 850 hPa. The variance in the large-scale domain of the NCEP analyses ($\mathcal{L}_g$) is roughly reproduced by both REMO runs, while the variances in the spatial domain well resolved by REMO but less well by NCEP ($\mathcal{S}_g \cap \mathcal{L}_r$) is markedly larger in both regional models than in the global analyses. In fact, the simulation with nudging is attaining even larger variances than the standard run.

Thus, the desired double effect—a greater similarity in the spectral range $\mathcal{L}_g \cap \mathcal{L}_r$ without a restriction of the variability on the smaller scales—is achieved in the spectral nudging run.

With the standard boundary forcing, episodes emerge with patterns quite dissimilar to the driving NCEP analysis. An example is the episode of 9–12 March, which is marked by low $\mathcal{P}_g$ similarity for the zonal wind (Fig. 5). In this situation (Fig. 6), a persistent high pressure system is placed in the center of the integration area, blocking the eastward propagation of synoptic disturbances. For example, the low pressure center initially located over Iceland moves northeastward and the trough west of Ireland moves toward the British Isles and is dissipated there. In the standard run, this trough is not dissipated as quickly and causes the central European high to be distorted. In the spectral nudging run, on the other hand, the overall evolution is similar to that of the NCEP reanalyses, but the details deviate to some extent.

The different evolutions are revealed by the different mean sea level air pressure distributions of the boundary forcing run and the NCEP analyses and of the spectral nudging run and NCEP analysis (Fig. 7). Clearly, the

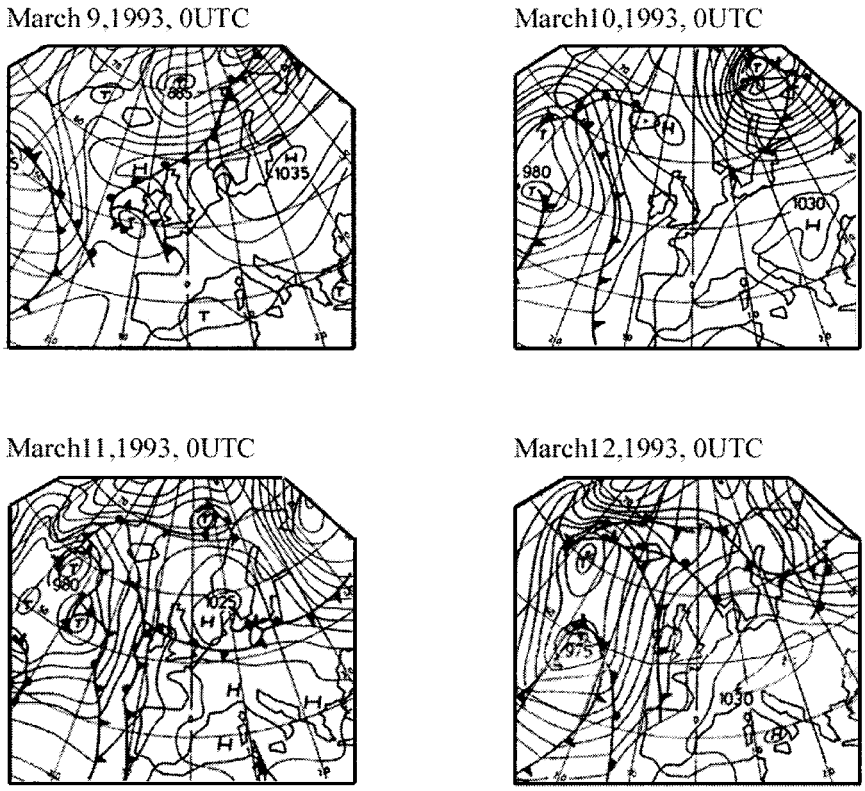

FIG. 8. Manually drawn mean sea level air pressure analyses from Berliner Wetterkarte, 9–12 Mar 1993

pressure field in the boundary forcing run deviates on large scales from NCEP. This is particularly striking on 12 March 1993, when over most of the Atlantic negative pressure deviations prevail. In the spectral nudging run, on the other hand, the differences arise at a smaller spatial scale. Also the magnitude of the differences in the boundary forcing run, reaching values of 15 hPa and higher in all maps of 9–12 March, is considerably larger than in the spectral nudging run, where only a few isolated maxima of about 10 hPa occur. Also in other variables, large deviations emerge (not shown). In terms of 850-hPa temperature, for instance, large-scale differences up to 10 K develop between the NCEP reanalyses and the standard run, whereas in the spectal nudging the differences are of much smaller spatial scale with maximum values of 4 K. Similarly, in 500-hPa geopotential height, differences of up to 300 m appear in the standard run compared to 50 m in the spectral nudging run.

A comparison with the manually drawn regional analyses of the Berliner Wetterkarte confirms that the the regional model with the boundary forcing only run has gone astray (Fig. 8). Some details, like the deepening of the small cutoff low over northern Norway, on 11 March, with a core air pressure of 1000 hPa in NCEP but 995 hPa in the spectral nudging run is confirmed by the Berliner Wetterkarte. Also the formation of two separate cyclones over the Atlantic on 12 March is a feature missing in the NCEP reanalyses but identified by the Berlin meteorologists.

We suggest that the 9–12 March evolution in the standard run takes place because the interior dynamics is not capturing the blocking situation prevailing in the large-scale state. Since this blocking is hardly encoded in the boundary conditions, the ''outer'' state given by NCEP and the ''inner'' state given by the standard REMO run become inconsistent. The spectral nudging technique, however, is efficient enough to keep the inner solution on the right trajectory.

Closer inspection of Fig. 7 reveals another positive feature of both REMO simulations, namely the small-scale features related to fronts, which are absent in the NCEP analyses but present in the Wetterkarten analysis of Fig. 8. Thus, the spectral nudging does not hamper the emergence of small-scale features.

An intercomparison in the frequency domain reveals that nudging dampens the regional model's tendency to develop its own low-frequency dynamics. Figure 9 shows autospectra and squared coherence spectra for mean sea level air pressure at the station of de Bilt, Netherlands, for the driving NCEP analysis (solid) and for the two REMO simulations (dashed). For time periods longer than about 3 days, the REMO standard run generates additional low-frequency variance, which is

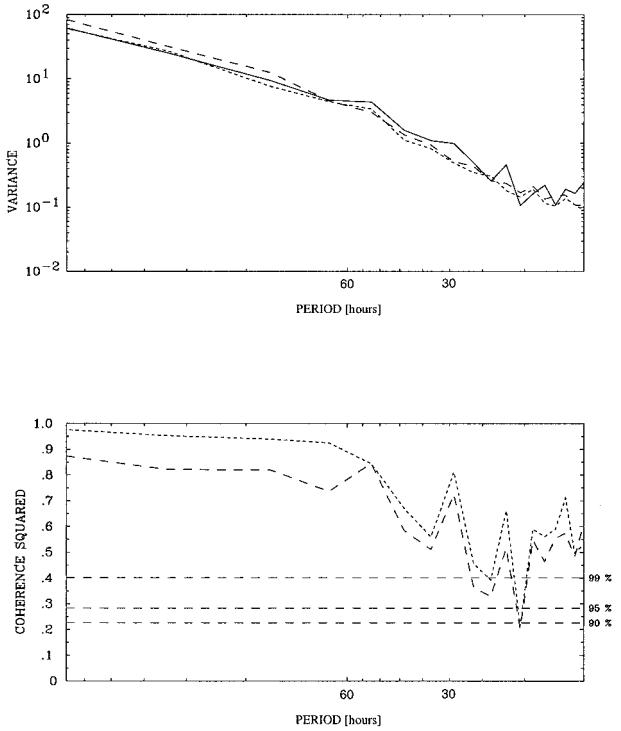

FIG. 9. Spectra of analyzed and REMO simulated mean sea level air pressure at the station in De Bilt, Netherlands. (top) Autospectra: the solid lines refer to the NCEP analyses, the long dashed line to the standard REMO run, and the short dashed line to the spectral nudging REMO run. (bottom) Squared coherency spectra: the long dashed line refers to the coherence between the NCEP analyses and the standard run, whereas the short dashed line represents the similarity of the spectral nudging run and the analyses.

suppressed by the nudging. At higher frequencies, both REMO simulations are rather similar. These findings are supported by the squared coherence spectra between the NCEP analyses and the REMO simulations; for time periods of 72 h and more, a much higher coherence is obtained for the spectral nudging run than for the standard boundary control run, whereas for shorter timescales, the coherence drops down and the regional model develops its own dynamics.

We made an additional simulation with summer conditions and found similar results, including episodes when the model with standard forcing develops a meteorologically plausible but not actually observed state.

b. Comparison with observational data

The two REMO runs (with standard boundary forcing and spectral nudging) and the NCEP reanalyses (only mean sea level air pressure and temperature) were compared against observed time series of mean sea level air pressure at a number of central European stations. Also, for the time period January–March 1993, wind observations from the oil field Ekofisk in the central North Sea were available, which are compared to the REMO simulations as well.

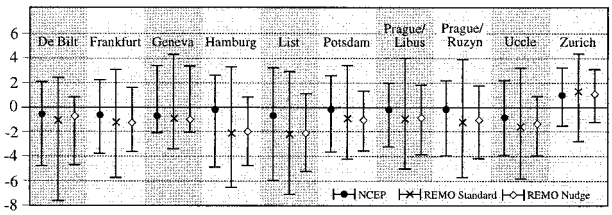

FIG. 10. Differences ''station data minus simulation'' for a series of central European stations and NCEP, REMO standard, and REMO spectral nudging. The variable considered is mean sea level air pressure. The center points represent the mean differences, and the bars indicate the range spanned by the 10% and 90% percentiles.

For air pressure at the 10 locations, REMO returns a bias of about 1 hPa for both formulations whereas NCEP has better mean values (Fig. 10). However, the spread of errors is considerably smaller in the case of the spectral nudging simulation.

Figure 11 displays time series of the meridional and zonal components of the wind at 10-m height at Ekofisk. Actually, the observations are taken at a higher altitude,

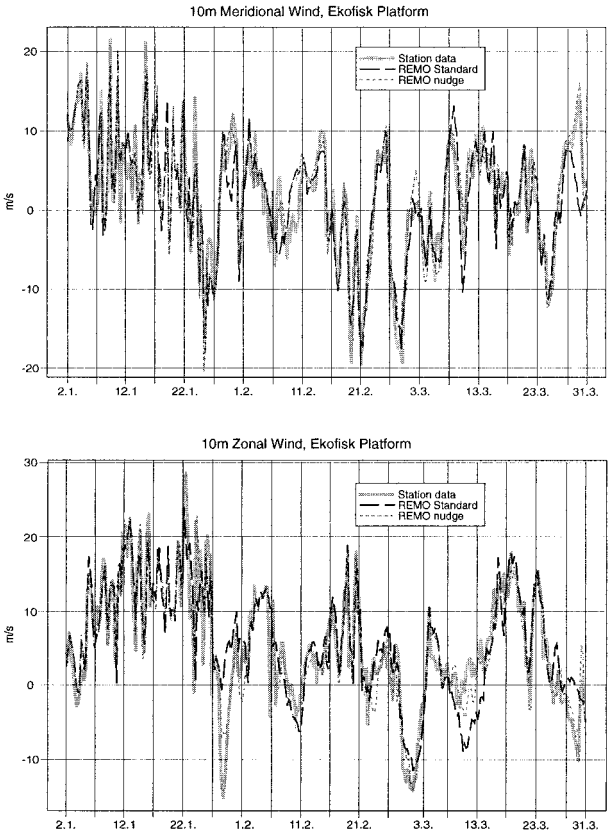

FIG. 11. Time series of meridional and zonal wind components at Ekofisk in the central North Sea from Jan to Mar 1993. The observed values are reduced to the standard height of 10 m: thick gray line, observations; light dashed continuous line, REMO spectral nudging; heavy dashed line, REMO standard.

TABLE 2. Time mean measures of similarity for zonal and meridional wind components at 500 hPa and for different strengths of spectral nudging.

Wind at 500 hPa	$\mathcal{P}_g$ α 0.1	$\mathcal{P}_g$ α 0.05	$\mathcal{P}_g$ α 0.025	$\mathcal{P}_g$ α 0	$\mathcal{P}_r$ α 0.1	$\mathcal{P}_r$ α 0.05	$\mathcal{P}_r$ α 0.025	$\mathcal{P}_r$ α 0
Zonal	0.996	0.994	0.991	0.931	0.344	0.325	0.304	0.216
Meridional	0.984	0.976	0.964	0.855	0.205	0.239	0.205	0.076

and the values are reduced to a standard height of 10 m through a standard calculation. All three curves coincide relatively well. A remarkable feature is that in many cases the maxima and minima of the wind components of the order of 20 m s^{-1} are reproduced. A closer inspection reveals intermittently significant deviations by the standard run and improvements in the spectral nudging run. The 9–12 March episode emerges clearly in the time series of the zonal wind.

c. Sensitivity experiments

Two additional simulations have been performed with different values of the nudging coefficient η^0. In one run, η^0 was doubled (i.e., $\alpha = 0.1$), in another simulation it was halved ($\alpha = 0.025$). In order to save computer time, the sensitivity experiments were done only for 1 month, starting with state of 1 March of the 3-month spectral nudging run considered so far.

We assess the sensitivity of the simulation to this choice by calculating the measures of similarity $\mathcal{P}_g$ and $\mathcal{P}_r$ as defined by (1) for scales well resolved by the NCEP reanalyses and by the REMO simulations only. The time mean measures of similarity, for the zonal and meridional wind components at 500 hPa, are listed in Table 2 for the different strengths of spectral nudging ($\alpha > 0$) as well as for the standard case ($\alpha = 0$).

The large-scale control seems to be exerted efficiently also by the other two choices of α, with markedly higher similarity measures. A more comprehensive study will be needed for designing an optimal configuration of the nudging technique, but this first sensitivity analysis indicates that the performance does not depend significantly on the choice of α.

5. Conclusions

In the present paper we have tested the spectral nudging technique, introduced by Waldron et al. (1996) into regional weather forecasting, in regional climate simulations. The spectral nudging concept deviates from the classical approach as the problem is not considered to be a boundary value problem in the gridpoint domain, but a downscaling problem. That is, the information that is processed in the model is not so much the state specified at the areal boundaries but at the large scales. In a generalized sense, this is again a boundary problem, but this time formulated in the spectral domain.

The purpose of the paper was not to delineate the optimal configuration of spectral nudging, but to demonstrate the concept, its feasibility, and its potential. Our key argument for the success of the spectral nudging technique is the observation that the nudging technique prevents the regional model to go astray for limited times, generating internal states inconsistent with the driving fields. We have demonstrated that this uncontrolled wandering is not merely a theoretical problem of the regional model forced from the boundaries, but really takes place (see also Rinke and Dethloff 2000). At the same time, the spectral nudging forcing does not impede the regional model's ability to develop regional- and small-scale features superimposed on the large-scale driving conditions.

Different purposes of models require different formulations. When dynamical aspects are to be addressed, such as the dynamics during the genesis of a storm, the spectral nudging should not be used, as it modifies the dynamics inasmuch as it introduces additional forcing terms into the momentum equation. Also, when a significant two-way coupling is expected to take place, as in the case of the life cycle of a hurricane, the spectral nudging will not be adequate. When, however, specifications of regional climate statistics are needed, such as in paleoclimatic and historic reconstructions and climate change applications, our technique should be preferred as it generates weather streams consistent with the large-scale driving fields.

Acknowledgments. We are thankful to the reviewers for substantial suggestions, to Daniela Jacob and Ralf Podzun for their help with the model, to Arno Hellbach for helping us access the NCEP data, to Lennart Bengtsson for permission to use the model, to Mariza Costa-Cabral and Beate Müller for advice, and to Reiner Schnur for the observational data. Beate Gardeike professionally prepared many of the diagrams. Ralf Weisse made the spectral analysis (Fig. 9) for us.

REFERENCES

Cocke, S., and T. E. LaRow, 2000: Seasonal predictions using a regional spectral model embedded within a coupled ocean-atmosphere model. *Mon. Wea. Rev.,* **128,** 689–708.

Davies, H. C., 1976: A lateral boundary formulation for multi-level prediction models. *Quart. J. Roy. Meteor. Soc.,* **102,** 405–418.

Doms, G., and Coauthors, 1995: Dokumentation des EM/DM-Systems. Deutscher Wetterdienst Abteilung Forschung, Offenbach,

Germany. [Available from Deutscher Wetterdienst, Zentralamt, Abteilung Forschung, Postfach 10 04 65, 63004 Offenbach a Main, Germany.]

Frey-Buness, F., D. Heimann, and R. Sausen, 1995: A statistical-dynamical downscaling procedure for global climate simulations. *Theor. Appl. Climatol.,* **50,** 117–131.

Fuentes, U., and D. Heimann, 1996: Verification of statistical-dynamical downscaling in the Alpine region. *Climate Res.,* **7,** 151–186.

Giorgi, F., 1990: On the simulation of regional climate using a limited area model nested in a general circulation model. *J. Climate,* **3,** 941–963.

——, M. R. Marinucci, and G. T. Bates, 1993: Development of second-generation regional climate model (RegCM2). Part II: Convective processes and assimilation of lateral boundary conditions. *Mon. Wea. Rev.,* **121,** 2814–2832.

Jacob, D., and R. Podzun, 1997: Sensitivity studies with the regional climate model REMO. *Meteor. Atmos. Phys.,* **63,** 119–129.

——, ——, and M. Claussen, 1995: REMO—A model for climate research and weather prediction. *Proc. Int. Workshop on Limited-Area and Variable Resolution Models,* Beijing, China, 273–278.

Juang, H.-M. H., and M. Kanamitsu, 1994: The NMC Regional Spectral Model. *Mon. Wea. Rev.,* **122,** 3–26.

——, S.-Y. Hong, and M. Kanamitsu, 1997: The NCEP Regional Spectral Model: An Update. *Bull. Amer. Meteor. Soc.,* **78,** 2125–2143.

Kalnay, E., and Co-authors, 1996: The NCEP/NCAR 40-Year Reanalysis Project. *Bull. Amer. Meteor. Soc.,* **77,** 437–471.

Kauker, F., 1998: Regionalization of climate model results for the North Sea. Ph.D. thesis, University of Hamburg, 109 pp. [Available from GKSS Research Center, Max-Planck-Str., 121502 Geesthacht, Germany.]

Kida, H., T. Koide, H. Sasaki, and M. Chiba, 1991: A new approach to coupling a limited area model with a GCM for regional climate simulation. *J. Meteor. Soc. Japan,* **69,** 723–728.

Kidson, J. W., and C. S. Thompson, 1998: Comparison of statistical and model-based downscaling techniques for estimating local climate variations. *J. Climate,* **11,** 735–753.

Kouker, W., D. Offermann, V. Küll, T. Reddemann, R. Ruhnke, and A. Franzen, 1999: Streamers observed by the CRISTA experiment and simulated in the KASIMA model. *J. Geophys. Res.,* **104** (D13), 16 405–16 418.

McGregor, J. L., J. J. Katzfey, and K. C. Nguyen, 1998: Fine resolution simulations of climate change for southeast Asia. Southeast Asian Regional Committee for START Research Project Final Report, 51 pp. [Available from CISRO Atmospheric Research, PMB 1, Aspendale, VIC 3195, Australia.]

Navarra, A., and K. Miyakoda, 1988: Anomaly general circulation models. *J. Atmos. Sci.,* **45,** 1509–1530.

Podzun, R., A. Cress, D. Majewski, and V. Renner, 1995: Simulation of European climate with a limited area model. Part II: AGCM boundary conditions. *Beitr. Phys. Atmos.,* **68,** 205–225.

Rinke, A., and K. Dethloff, 2000: The influence of initial and boundary conditions on the climate of the Arctic in a regional climate model. *Climate Res.,* **14,** 101–113.

Sasaki, H., J. Kida, T. Koide, and M. Chiba, 1995: The performance of long term integrations of a limited area model with the spectral boundary coupling method. *J. Meteor. Soc. Japan,* **73,** 165–181.

von Storch, H., 1995: Inconsistencies at the interface of climate impact studies and global climate research. *Meteor. Z.,* **4,** 72–80.

——, 1999: The global and regional climate system. *Anthropogenic Climate Change,* H. von Storch and G. Flöser, Eds., Springer-Verlag, 3–36.

——, M. Costa-Cabral, F. Feser, and C. Hagner, 2000: Reconstruction of lead (Pb) fluxes in Europe during 1955–1995 and evaluation of gasoline lead-content regulations. Preprints, *11th Joint Conf. on the Applications of Air Pollution Meteorology,* Long Beach, CA, Amer. Meteor. Soc. and Air and Waste Management Association, 324–329.

Waldron, K. M., J. Peagle, and J. D. Horel, 1996: Sensitivity of a spectrally filtered and nudged limited area model to outer model options. *Mon. Wea. Rev.,* **124,** 529–547.